Reprinted from

NUCLEAR PHYSICS, VOLUME 40 No. 4 (1963)

E. MATTHIAS, L. BÖSTROM, ALICE MACIEL, M. SALOMON
and T. LINDQVIST

MAGNETIC DIPOLE INTERACTION STUDIED BY THE DIFFERENTIAL ANGULAR CORRELATION METHOD

NORTH-HOLLAND PUBLISHING COMPANY - AMSTERDAM

PRINTED IN THE NETHERLANDS

1.E.3:
6.A

Nuclear Physics **40** (1963) 656—669; © *North-Holland Publishing Co., Amsterdam*

MAGNETIC DIPOLE INTERACTION STUDIED BY THE DIFFERENTIAL ANGULAR CORRELATION METHOD

E. MATTHIAS, L. BOSTRÖM, ALICE MACIEL †, M. SALOMON †† and T. LINDQVIST
Institute of Physics, University of Uppsala, Uppsala, Sweden

Received 27 August 1962

Abstract: An apparatus for the investigation of differential angular correlations between two gamma rays is described. The principles of g-factor measurements with the differential method are analysed, taking into account the influence of the finite resolving time of the time-to-pulse-height converter and the influence of time-dependent perturbations. Using this method, the following g-factors have been re-determined:

$g = +1.29 \pm 0.02$ for the 482 keV state in Ta^{181},

$g = -0.318 \pm 0.007$ for the 247 keV state in Cd^{111}.

1. Introduction

The investigation of γ-γ angular correlations perturbed by an interaction between electric and magnetic moments of the intermediate state and extranuclear fields makes it possible, under certain conditions, to determine nuclear moments experimentally [1-3]). It is mainly the magnetic dipole interaction which has been used for such experiments due to the fact that external magnetic fields of sufficient strength can be obtained under controlled conditions. The interaction between a magnetic field and the magnetic dipole moment of a nuclear state gives rise to a Larmor precession with frequency $\omega_L = gB\mu_N/\hbar$, where g is the nuclear g-factor and B is the magnetic field strength. The frequency ω_L can be obtained from an investigation of the behaviour of the angular correlation pattern of two cascading gamma rays in an external magnetic field.

The unperturbed angular correlation function of a gamma cascade can be written as

$$W(\theta) = \sum_{k \text{ even}} A_k P_k(\cos\theta). \tag{1}$$

If a magnetic field is applied perpendicular to the plane of the detectors the angular correlation function becomes time-dependent:

$$w(\theta, \omega_L, t) = \sum_{k \text{ even}} g_k(t) A_k P_k[\cos(\theta \pm \omega_L t)], \tag{2}$$

the plus and minus signs referring to opposite field directions. A possible time-

† On leave from Instituto de Fisica, U.R.G.S., Porto Alegre, Brasil.
†† On leave from Instituto de Fisica, C.N.E.A., Bariloche, Argentina.

dependent perturbation in the source is taken into account by the differential attenuation factor

$$g_k(t) = \exp(-\lambda_k t), \tag{3}$$

where λ_k is the relaxation constant of the internal perturbation [4]). Expression (2) shows that the angular correlation pattern rotates with a precession angle $\Delta\theta = \omega_L t$ which depends on the lifetime t of each individual intermediate state.

The experimental equipment for angular correlation studies includes, however, a coincidence circuit with a finite resolving time $2\tau_0$, the size of which compared to the nuclear lifetime τ_N determines the method by which ω_L can be obtained. Historically, one started with a coincidence system with long resolving time, i.e. $2\tau_0 \gg \tau_N$. In this approach the correlation function is given by

$$W(\theta, \omega_L) = \lambda \int_0^\infty w(\theta, \omega_L, t) \exp(-\lambda t)\mathrm{d}t. \tag{4}$$

The evaluation of the integral leads to

$$W(\theta, \omega_L) = 1 + \tfrac{1}{4} A_2 G_2 \left\{1 + \frac{3\cos 2(\theta - \Delta\theta_{22})}{[1+(2\omega_L \tau_N G_2)^2]^{\frac{1}{2}}}\right\} + \tfrac{1}{64} A_4 G_4 \left\{9 + \frac{20\cos 2(\theta - \Delta\theta_{24})}{[1+(2\omega_L \tau_N G_4)^2]^{\frac{1}{2}}} + \frac{35\cos 4(\theta - \Delta\theta_{44})}{[1+(4\omega_L \tau_N G_4)^2]^{\frac{1}{2}}}\right\}, \tag{5}$$

where the displacement angles $\Delta\theta_{jk}$ are defined by

$$\Delta\theta_{jk} = j^{-1}\mathrm{arctg}\, j\omega_L G_k \tau_N, \qquad 0 < \Delta\theta_{jk} < \pi/2j, \qquad j = 2, 4. \tag{6}$$

In eq. (5) the quantities $G_k = (1+\lambda_k \tau_N)^{-1}$ are the integral attenuation factors.

The integral correlation method has been used by several groups and has led to valuable information about the magnetic properties of nuclear excited states. The accuracy in the determination of ω_L, however, is limited by the fact that the total displacement angle of the correlation pattern is restricted as indicated in eq. (6). Only in most favourable cases the limits of error can be reduced to 3%, which means that the total displacement angle has to be determined to about $\pm 1°$. Another drawback in the integral method is that any time-dependent perturbation causes the occurrence of a k-dependent precession frequency $\omega_{Lk}^{\mathrm{eff}} = \omega_L G_k$. In order to obtain the pure Larmor frequency, G_k or λ_k must be determined in a separate measurement.

These two difficulties are eliminated in the differential angular correlation method [5, 6]). By choosing $2\tau_0 \ll \tau_N$ it is possible to obtain $w(\theta, \omega_L, t)$ in its periodic time behaviour by investigating the time spectrum of the coincidence rate given by

$$C(\theta, \omega_L, t) = \text{const.} \exp(-t/\tau_N) w(\theta, \omega_L, t). \tag{7}$$

Obviously, the time spectrum shows an exponential decay pattern "modulated" by the correlation function $w(\theta, \omega_L, t)$. The modulation pattern depends on the form

of the correlation function. In the case of a dominant A_2 term, the modulation amplitude has two maxima and two minima for each complete turn of the spin axis rotation. If the angular correlation is given mainly by the A_4 term, the number of maxima and minima is doubled.

The main advantage of this method is the fact that the spin axis precession can be followed during several turns. Thus, the displacement angle $\Delta\theta$ is large and can be obtained with small relative error. Furthermore, the detectors are in fixed positions and the angle between them does not have to be known with high precision. Any additional time-dependent perturbation shows up in an exponentially decreasing modulation amplitude, but it does not affect the periodicity of the modulation. Thus, the pure Larmor frequency ω_L can be obtained directly and there is no need for an additional independent investigation of the time-dependent perturbation.

The principle of the differential angular correlation method has been known from the beginning of perturbed correlation measurements. One of the first differential experiments was done by Lehman and Miller [7]) who measured the electric quadrupole interaction in a metallic In^{111} source by using a coincidence resolving time $2\tau_0 < \tau_N$ and various delays. However, statistical reasons did not allow many delay experiments to be done before the appearance of multichannel analysers. As pointed out in ref. [6]) the use of time-to-pulse-height converters in combination with multichannel analysers removes these difficulties and makes the differential method a powerful tool for halflives longer than a few nanoseconds. The possibilities of this method seem now to have attracted the interest of many groups. M. Deutsch *et al.* [5]) had used the method for a measurement of the g-factors of the 482 keV level in Ta^{181} and of the 81 keV level in Cs^{133}. Recently, Bożek *et al.* [8]) also reported a measurement of the g-factor of the 482 keV state in Ta^{181} by the differential method. Bergström and Thieberger [9]) have used the same method for determining the magnetic moment of the first excited state in Sc^{44}.

In this paper we want to discuss some experimental details in connection with the differential method together with g-factor measurements for Ta^{181} and Cd^{111}.

2. Apparatus

2.1. GENERAL DESCRIPTION

As shown in the block scheme in fig. 1 the apparatus consists of two single-channel analysers, a time-to-pulse-height converter (TPHC), a multichannel analyser and a magnet. The photomultiplier tubes of type RCA-6342A are operating at a high voltage of about +2300 V. The anode pulses of the photomultipliers are applied directly to the grids of the E 810 F limiter tubes which are working with a quiescent plate current of 35 mA. The limiter pulses go to the TPHC and to the coincidence circuit. The "slow" pulses are taken from the 5th dynode and fed to the amplifiers and single-channel analysers. A RIDL 400-channel analyser has been employed for the measurements.

The TPHC is a modified version of the well-known Green-Bell circuit [10]). The limiter pulses, going to the 6BN6 tube to overlap, are clipped to a length of 100 ns and occasionally pulse lengths up to 200 ns have been used. The coincidence circuit, also a 6BN6 tube, operating at a plate voltage of 35 V is fed with the same limiter pulse from the delayed side (second gamma ray) and from the prompt side (first gamma ray) with a short pulse of 8 ns taken from the end of the reflection cable

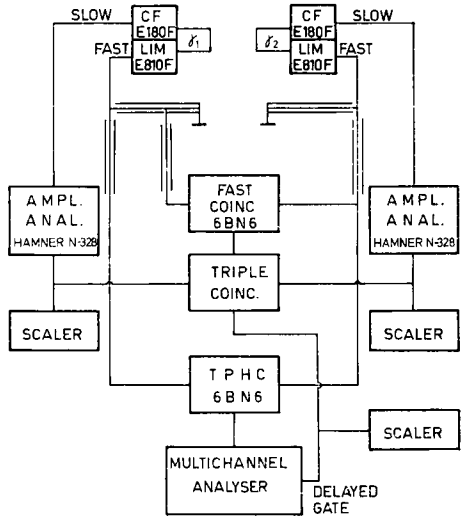

Fig. 1. Block scheme for a differential angular correlation apparatus.

(fig. 1). Through suitable delays this short pulse is put at the rear end of the second pulse, when the two signals are prompt. For delayed signals there is still a coincidence overlap within the length of the delayed pulse which in this way determines the time region of the converter. Using the 6BN6 tube, a single to coincidence ratio of better than 1:10 is obtained even for signals which differs in length by a factor of 10 or more. A special high stabilized DC power supply has been used for the filaments of the TPHC and the coincidence unit. During a measurement filament and DC voltages were checked with a graphical recorder. The coincidence pulses are amplified and selected by a discriminator. The signals from the coincidence circuit and the two signals from the pulse-height analysers are fed into a triple coincidence circuit of Garwin type [11]). The output from this triple coincidence circuit is then used as a gating signal to the multichannel analyser for the pulses from the TPHC.

2.2. TIME CALIBRATION AND PERFORMANCE OF TPHC

The TPHC has been time calibrated with the known delay time of various lengths of RG-63 B/U cables. The time delays of the cables have been measured carefully by observing destructive interference of hf-wave trains in open-end and short circuited

cables. Interference minima will occur for $T = n/2f$ and $T = (n+\frac{1}{2})/2f$ in the first and second case, respectively. Here, f is the frequency of the hf-generator, T is the time delay of the cable and $n = 1, 2, 3, \ldots$. In practice, it is necessary to normalize the measured amplitude with the amplitudes observed for a matched cable. A plot of the number of minima obtained versus the frequency of the hf-generator shows a straight line, the slope of which gives the delay time T of the cable.

Obviously, the accuracy of the delay time measurement is given by the number of minima which is possible to obtain. This number is limited by the length of the cable and the damping factor for high frequencies. As an example it will be mentioned that 24 minima between 10 MHz and 125 MHz have been observed in a RG-63 B/U cable of 26m length giving a delay of 4.00 ± 0.01 ns/m. The delay time of the various delay cables has been measured separately. After a check of the hf-generator against a frequency standard the final time calibration of TPHC could be done with an accuracy of better than 1%.

To check the performance of TPHC the well-known halflife of the 482 keV level in Ta^{181} was measured. Special care was taken to avoid the influence of a time-dependent electric quadrupole perturbation [12]). Thus, the angle between the two detectors was chosen to about 140°, and one detector was moved up very close to the source to smear out any remaining angular correlation. The result for the halflife of the 482 keV level in Ta^{181} was

$$T_{\frac{1}{2}} = 11.0 \pm 0.1 \text{ ns},$$

which is in agreement with recent results [13]).

2.3. MAGNET

A conventional, watercooled electromagnet was used. A field strength of 32 000 G could be obtained in a 6 mm air gap. The homogeneity of the field was better than 1.5% over a diameter of 5 mm. The field strength was measured with a small test coil and a fluxmeter, which assembly was calibrated in an NMR equipment. The overall accuracy of the field measurement, corrected for inhomogeneity, is found to be better than 1%, and will add to the limits of error for the final g-factor value. It would be much more favourable to use a nuclear resonance arrangement for the field determination, the inhomogeneity and the smallness of the interesting volume, however, introduce technical difficulties. During a run, which could take 12-24 hours, the constancy of the magnetic field was checked with a Hall-plate inserted nearby the source position. The voltage from the Hall plate was recorded continuously on a graphical recorder.

3. Treatment of Data

3.1. SPECIFIC FORMULATION

In principle $C(\theta, \omega_L, t)$ of eq. (7) can be used for evaluating ω_L. However, in order to eliminate the exponential decay and to obtain quantities more sensitive to

the modulations one can combine the results from "field up" and "field down" measurements C^+ and C^-. Further one can choose between measuring only at one fixed angle θ_0 or at two angles, θ_1 and θ_2, as done by Bożek *et al.* [8]). We preferred the one-angle method, because it does not require a large accuracy in the source adjustment and the detector arrangement is fixed. Forming the ratio

$$R = 2\frac{C^+ - C^-}{C^+ + C^-} \tag{8}$$

and inserting eqs. (7) and (2) one obtains with $\theta_0 = 135°$

$$R(t) = \frac{(12A_2 + 5A_4)\sin 2\omega_L t}{8 + 2A_2 + \frac{1}{8}A_4(9 - 35\cos 4\omega_L t)}\,. \tag{9}$$

3.2. INFLUENCE OF FINITE RESOLVING TIME

Eq. (9) is valid for an infinitely short time resolution of the converter circuit. In practice, this can be realized approximately only for longer halflives and even here only if the γ-energies are sufficiently large. The influence of the finite resolving time $2\tau_0$ is obviously a smearing out of the amplitude of $R(t)$. This corresponds to the effect of the finite solid angle of the detectors in ordinary angular correlation work. The influence of $2\tau_0$ is taken into account by integrating the coincidence counting rate $C(t)$ (eq. (7)) in each point t_i over the proper form of the prompt resolution curve $\varepsilon(t)$ which extends from $t_1 \leqq t \leqq t_2$:

$$C_{\mathrm{int}}(t_i) = \int_{t_1}^{t_2} \sum_k \exp\left[-(\lambda + \lambda_k)t\right] A_k P_k[\cos(\theta - \omega_L t)]\varepsilon(t)\mathrm{d}t. \tag{10}$$

The difficulty is to evaluate these integrals, since the exact analytical form of the prompt resolution curve is not known. Hitherto, only the cases (a) rectangular resolution interval and (b) Gaussian shape of the prompt curve [14]) have been considered.

It is expected that the influence of $2\tau_0$ on the amplitude of $R(t)$ shows the same tendency in both cases, therefore we found it sufficient to discuss only case (a). Furthermore, the solution of the integral (eq. (10)) can then mathematically be expressed in a closed form which is not possible in case (b). The integrated ratio $R(t)$ is discussed only for $t_i \geqq \tau_0$ because a rectangular time resolution interval is not expected to describe the situation very well in the region of the prompt curve.

Thus, taking $\varepsilon(t)$ as

$$\varepsilon(t) = \begin{cases} 1 & \text{for } t_i - \tau_0 \leqq t \leqq t_i + \tau_0 \\ 0 & \text{for } t_i - \tau_0 > t,\ t_i + \tau_0 < t, \end{cases} \tag{11}$$

the integration of eq. (10) for $t_i \geqq \tau_0$ yields for $\theta_0 = 135°$, replacing t_i by t

$$R(t) = \frac{[3A_2' B_{22} + \frac{5}{4}A_4' B_{24}] \cos 2\omega_L t - [3A_2' C_{22} + \frac{5}{4}A_4' C_{24}] \sin 2\omega_L t}{2 \sinh \lambda\tau_0 + \frac{1}{2}A_2' \sinh(\lambda+\lambda_2)\tau_0 + \frac{1}{32}A_4'[9 \sinh(\lambda+\lambda_4)\tau_0 - 35(C_{44} \cos 4\omega_L t + B_{44} \sin 4\omega_L t)]},$$

$$B_{jk} = \frac{1}{1+(j\omega_L \tau_N G_k)^2}[\sin j\omega_L \tau_0 \cosh(\lambda+\lambda_k)\tau_0 - j\omega_L \tau_N G_k \cos j\omega_L \tau_0 \sinh(\lambda+\lambda_k)\tau_0],$$

$$C_{jk} = \frac{1}{1+(j\omega_L \tau_N G_k)^2}[\cos j\omega_L \tau_0 \sinh(\lambda+\lambda_k)\tau_0 + j\omega_L \tau_N G_k \sin j\omega_L \tau_0 \cosh(\lambda+\lambda_k)\tau_0],$$

$$A_k' = A_k G_k \exp(-\lambda_k t). \tag{12}$$

The evaluation of the integrals leads to rather complicated expressions and the result is of approximate character only. These difficulties can be removed by representing the prompt resolution curve by a step function $\varepsilon(t)$. In this case the integration is transformed to a summation over the proper time intervals, the weight factors of which are given by the form of the prompt curve [15]). By choosing a large number of steps for $\varepsilon(t)$ this treatment will be a very good approximation. If the prompt curve is spread out over a sufficiently large number of channels, the channel width can be taken as the steps of $\varepsilon(t)$ and the counting rates of the prompt curve as the weighting factors.

3.3. BEHAVIOUR OF $R(t)$

The most important consequence of the integration (cf. eq. (12)) is that neither the finite resolving time nor a time-dependent perturbation affects the frequency of $R(t)$. The Larmor frequency ω_L can thus be obtained directly from the periodicity of $R(t)$. However, the amplitude of $R(t)$, which is affected by A_k, ω_L, τ_0 and λ_k, is also of interest for two reasons. Firstly the accuracy of the experimental determination of ω_L depends on the size of the amplitude, and secondly with the known quantities τ_0, λ and ω_L, the coefficients A_k and the relaxation constants λ_k can be evaluated from the measured amplitude of $R(t)$.

In order to study the influence of $2\tau_0$ and λ_2 separately, the following two cases are chosen: (1) $\lambda_2 = 0$, i.e. no time dependent perturbation, taking τ_0 and A_2 as a parameter, (2) $\tau_0 = \text{const.}$, taking λ_2 as a parameter, in both cases $A_4 = 0$.

The first case is demonstrated in fig. 2. There the amplitude of $R(t)$ is plotted as a function of the Larmor frequency ω_L for some values of $2\tau_0$ and the correlation coefficient A_2. In general, the amplitude is seen to decrease with increasing ω_L and increasing $2\tau_0$. For larger resolving times $2\tau_0$ and reasonable values of ω_L the curves show a slightly periodic behaviour with decreasing amplitude for increasing ω_L. This gives the interesting aspect that a modulation experiment with a smaller but still measurable amplitude should be possible even for larger values of ω_L, where the precession period $T_L = 2\pi/\omega_L$ is about the same or still smaller compared to the resolving time $2\tau_0$.

The second case, $\tau_0 = \text{const.}$, is shown in fig. 3, where $R(t)$ is plotted for some relaxation parameters. The function $R(t)$ behaves like a damped oscillation for $\lambda_2 \neq 0$, the larger λ_2 the stronger damping. Thus, if the experimentally determined $R(t)$ is constant this proves that no time-dependent pertubation is present in the source.

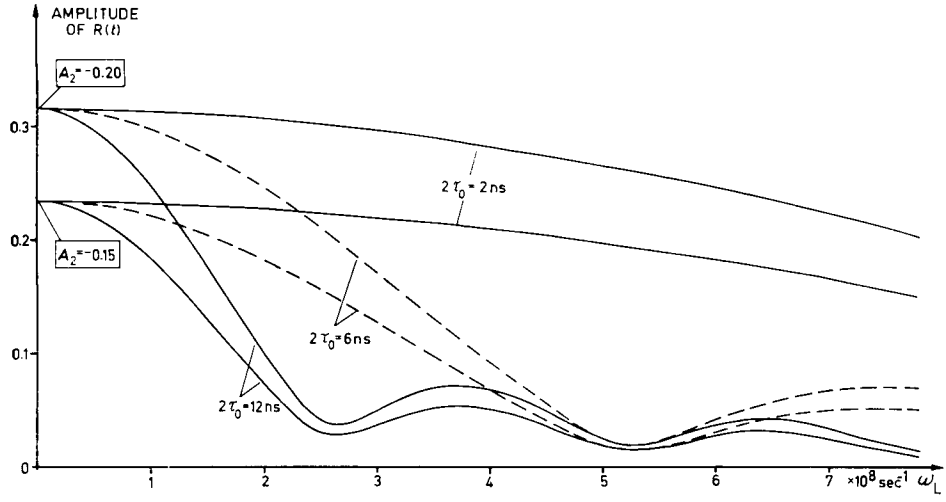

Fig. 2. Variation of the amplitude of $R(t)$ as a function of ω_L for $k_{max} = 2$, $\theta_0 = 135°$, $\tau_N = 15.8$ ns and $\lambda_2 = 0$. The resolving time $2\tau_0$ and the coefficient A_2 are taken as parameters.

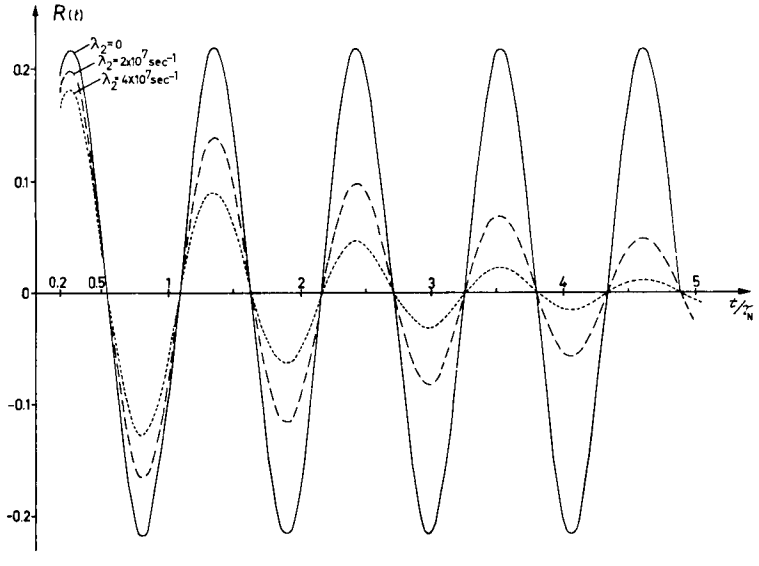

Fig. 3. Influence of a time-dependent perturbation on $R(t)$. The theoretical curves are plotted as a function of t/τ_N for $k_{max} = 2$, $\theta_0 = 135°$, $\tau_N = 15.8$ ns, $2\tau_0 = 6$ ns and $A_2 = -0.17$. The different parameters λ_2 correspond in the case of the 482 keV level of Ta^{181} to the integral attenuation factors $G_2 = 1$, $G_2 = 0.77$ and $G_2 = 0.62$, respectively.

4. Experimental Results

Although the differential method is from both a theoretical and a experimental point of view straightforward, we felt that the possibilities, the limitations, and the experimental details of the method had to be investigated with well-known cases. We therefore chose to start with the 482 keV level ($T_{\frac{1}{2}} = 11$ ns) in Ta^{181} and the 247 keV level ($T_{\frac{1}{2}} = 85$ ns) in Cd^{111}. These two isotopes are classic cases in the history of angular correlations and our results can then be compared with a big number of earlier results. The interesting parts of the decay schemes in this connection are shown in fig. 4.

4.1. POSSIBLE TIME-DEPENDENT PERTURBATION IN THE Hf SOURCE

It is well known that the electric quadrupole interaction is small if liquid HfF_4 sources are used. Our Hf source was obtained by dissolving HfO_2 (neutron-irradiated

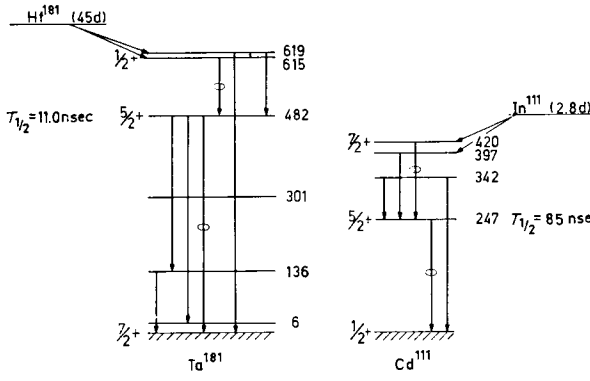

Fig. 4. Decay schemes of Hf^{181} and In^{111}.

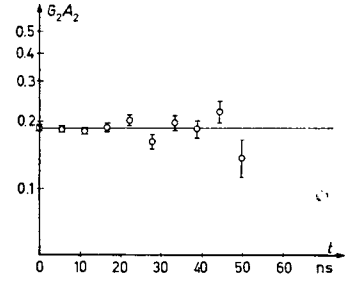

Fig. 5. Experimental investigation of a possible time dependency of the correlation coefficient $A_2G_2(t)$ of the 133 keV-482 keV cascade in Ta^{181} measured with a liquid HfF_4 source.

natural oxide) in 26-N HF. In order to investigate whether any time-dependent perturbation existed in this source a delayed correlation experiment was carried out using the angles $\theta = 90°$, 135° and 180°. In fig. 5 the experimental results for $A_2G_2(t)$

are shown. Each point is the sum of 20 channels in the multichannel analyser. As the experimentally determined quantity $\log G_2 A_2 = \text{const.} - \lambda_2 t$ is a constant, it can be

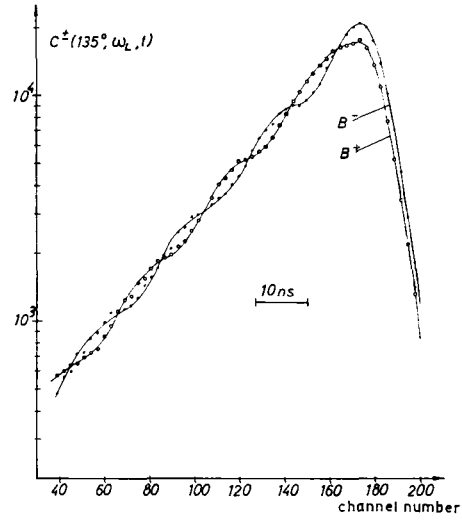

Fig. 6. Coincidence counting rate $C^{\pm}$ for the 133 keV-482 keV cascade in Ta^{181} and a magnetic field strength of about 31 kG. The resolving time was $2\tau_0 = 7.0$ ns.

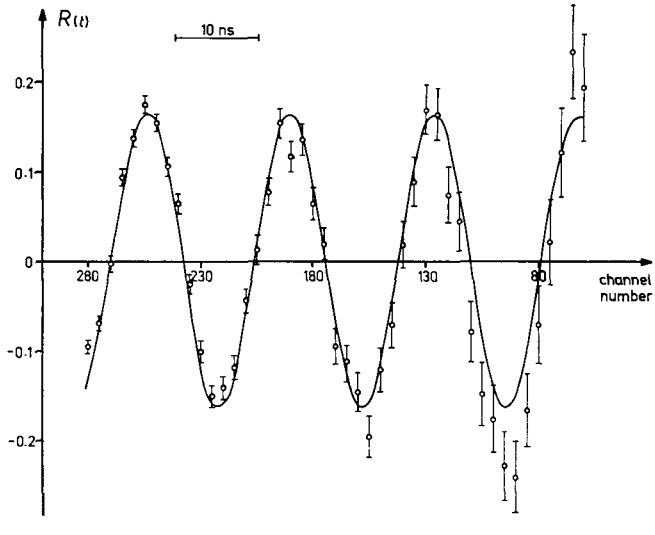

Fig. 7. $R(t)$ calculated for a measurement of Ta^{181} (source 1). The full line represents the weighted least square fit to the experimental points.

concluded that $\lambda_2 \approx 0$. The measured $G_4 A_4$ gave the same result ($\lambda_4 \approx 0$), however, the relative errors were big. Thus, it was concluded that the used Hf source was not

disturbed by any time-dependent perturbation, a fact that later should be confirmed by the behaviour of $R(t)$.

4.2. LARMOR FREQUENCY OF 482 keV STATE IN Ta^{181}

An external magnetic field of about 30 kG was applied to the Hf-source and the coincidence rates $C(\theta_0 = 135°, \omega_L, t)$ were measured for both up and down field directions. Two different sources were investigated. Before and after each run the resolving time and the position of the prompt curve were checked. Channel settings have been controlled with regular intervals during the run. A separate run for the determination of the accidental coincidences have been carried out with the "two-source" method, taking care in obtaining the same counting rates as in the main run.

A typical result for a run is shown in fig. 6. The resolving time of the TPHC in this case was 7.0 nsec using NaI(Tl) crystals on 20 cm long light guides. The A_2 term is dominant, and therefore (see eq. (2)) the modulation frequency of the C^+ and C^- curves is twice the Larmor frequency. From fig. 6 it can therefore be concluded that a total spin axis precession of about $1\frac{1}{2}$ turns have been observed. The sum of C^+ and C^- was plotted (not shown here) and gave exactly the right lifetime as found earlier. For the evlauation of the Larmor frequency eq. (12) has been used in the form $A\cos(\varphi - 2\omega_L t) + S_0$, which is obtained if the A_4 term is negligible and $\lambda_2 \approx 0$. The quantities ω_L, A, φ and S_0 are calculated by a least square fit (fig. 7).

TABLE 1

Results for the g-factor measurement for the 482 keV level in Ta^{181}

Source number	Magnetic field (G)	$2\tau_0$ (ns)	g
1	29800	7.6	1.276 ± 0.021
2	32050	5.5	1.281 ± 0.016
		Mean value:	1.279 ± 0.019

In table 1 the results of the two sources investigated are given. After a diamagnetic correction of 1/0.991 the g-factor of the 482 keV state in Ta^{181} was found to be

$$g = 1.29 \pm 0.02.$$

The quoted error include uncertainties in the magnetic field measurement (1 %), time calibration and instability (1 %).

As mentioned above there are quite a few earlier experimental determinations of this g-factor. The results obtained so far are shown in fig. 8. All results do not agree within their limits of error. However, it is believed that in some of the integral method experiments a time-dependent interaction may have been present, which is not corrected for. The deviation of the present result from the earlier differential measurements [5, 8]) remains unexplained.

4.3. LARMOR FREQUENCY OF 247 keV STATE IN Cd^{111}

A similar experiment as described above was carried out for the 173-247 keV cascade in Cd^{111}. Natural cadmium metal was irradiated with 6 MeV protons in the cyclotron of the Nobel Institute, Stockholm. The indium radioactivity from the reaction Cd(p, n)In was separated and dissolved in concentrated nitric acid, the

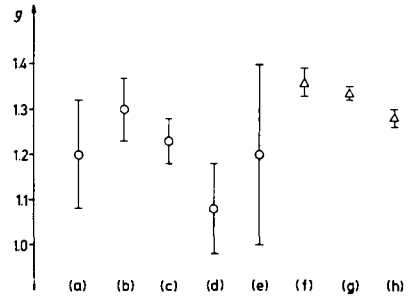

Fig. 8. Survey of experimental results for the g-factor of the 482 keV level in Ta^{181}. Circles refer to measurements done with the integral method, triangles to measurements with the differential method. The indicated points correspond to the following refs.: (a) ref. [16]), (b) ref. [17]), (c) ref. [18]), (d) ref. [19]), (e) ref. [20]), (f) ref. [5]), (g) ref. [8]), (h) present result.

solution constituting the source material. The half-life of the 247 keV state has earlier been determined [12]) to be $T_{\frac{1}{2}} = 85$ ns. In fig. 9 the result of the measurement is shown. Due to the limited time region of about 150 nsec 1 turn of the spin precession

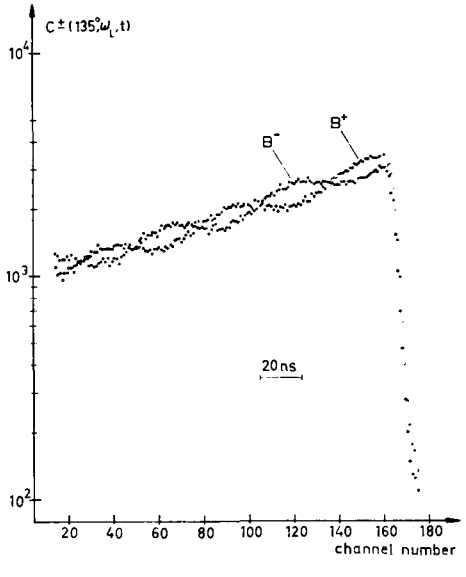

Fig. 9. Coincidence counting rate $C^{\pm}$ for the 173 keV - 247 keV cascade in Cd^{111} and a magnetic field strength of 32 600 G. The resolving time was $2\tau_0 = 6.6$ ns.

could be obtained in a magnetic field of 32600 G. The prompt time resolution was 6.6 nsec. The ratio $R(t)$ corresponding to this measurement is plotted in fig. 10.

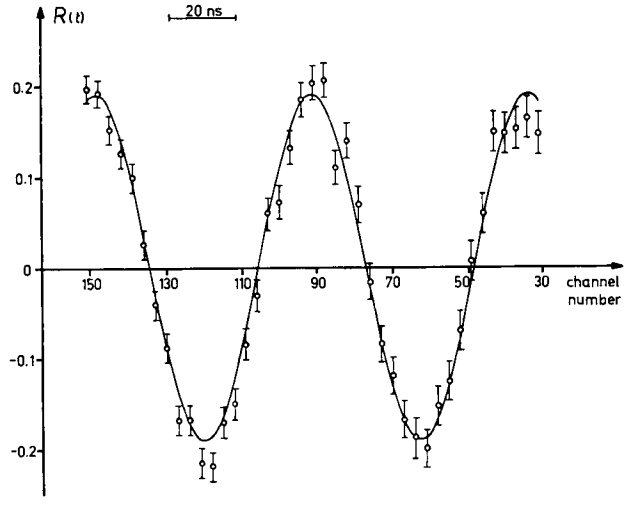

Fig. 10. $R(t)$ calculated for the measurement shown in fig. 9. The full line represents the weighted least square fit to the experimental points.

The amplitude of $R(t)$ remains constant within the limits of error and it can therefore be concluded that no time-dependent perturbation is present in the Cd source used. The result, including a diamagnetic correction of 1/0.995, was

$$g = -0.318 \pm 0.007.$$

The sign of the g-factor can be obtained from the rotation sense of the correlation pattern. Comparing the modulation curves in figs. 6 and 9 it can be seen, that the

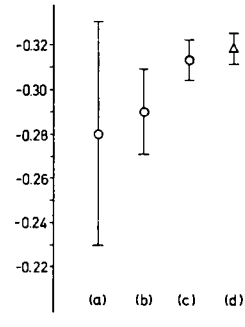

Fig. 11. Survey of experimental results for the g-factor of the 247 keV state in Cd^{111}. Circles refer to measurements done with the integral method, triangles to measurements with the differential method. The indicated points correspond to the following refs: (a) ref. [21]), (b) ref. [22]), (c) ref. [23]), (d) present result.

magnetic moments of the 482 keV level in Ta^{181} and of the 247 keV level in Cd^{111} have different signs (A_2 is negative in both cases). It should be noted, that the sign of the g-factor can only be obtained from the modulation pattern if the detectors are not placed at the angles $\frac{1}{2}\pi$, π and $\frac{3}{2}\pi$. For these detector positions the modulation structures for plus and minus field are identical.

A summary of all g-factors measured so far for the 247 keV level in Cd^{111} is shown in fig. 11. The present result agrees well with the previous reported value of Steffen and Zobel [23]).

The authors are very much indebted to Professor Kai Siegbahn for his interest in this work. Two of the authors (Alice Maciel and Martin Salomon) want to express their gratitude to the Swedish Agency for International Assistance for fellowships through the International Seminar for Research and Education in Physics. Financial support from The Swedish Atomic Research Council and a grant from the American Academy of Arts and Sciences are gratefully acknowledged. The investigation was financially supported by the US Air Force EOAR.

References

1) H. Frauenfelder, in Beta and gamma ray spectroscopy, ed. by K. Siegbahn (North-Holland Publ. Co., Amsterdam, 1955)
2) R. M. Steffen, Phil. Mag. Suppl. **4** (1955) 293
3) E. Heer and T. B. Novey, in Solid state physics, Vol. **9** ed. by F. Seitz and D. Turnbull (Academic Press, New York, 1959)
4) A. Abragam and R. V. Pound, Phys. Rev. **92** (1953) 943
5) M. Deutsch, A. Z. Hrynkiewicz and R. F. Stiening, MIT, Laboratory for Nuclear Science Progress Report, November 1959 (unpublished)
6) E. Matthias and T. Lindqvist, Nucl. Instr. and Meth. **13** (1961) 356
7) P. Lehman and J. Miller, J. Phys. et Rad. **17** (1956) 526
8) E. Bożek, A. Z. Hrynkiewicz and J. Styczen, Phys. Lett. **1** (1962) 126
9) I. Bergström and P. Thieberger, Ark. Fys. **22** (1962) 307
10) R. E. Green and R. E. Bell, Nucl. Instr. **3** (1958) 127
11) R. L. Garwin, Rev. Sci. Instr. **24** (1953) 618
12) P. C. Simms and R. M. Steffen, Phys. Rev. **108** (1957) 1459
13) T. D. Nainan, Phys. Rev. **123** (1961) 1751
14) E. Bodenstedt, H. J. Körner, G. Günther and J. Radeloff, Nuclear Physics **22** (1961) 145
15) J. Radeloff, private communication
16) S. Raboy and V. E. Krohn, Phys. Rev. **95** (1954) 1689
17) E. Heer, R. Rüetschi and P. Scherrer, Naturforsch. **10a** (1955) 834
18) V. E. Krohn and S. Raboy, Phys. Rev. **107** (1957) 536
19) T. Lindqvist and E. Karlsson, Ark. Fys. **12** (1957) 519
20) A. K. Walter, I. I. Zaliubovskii and W. A. Kliucharev, Conf. on Nuclear Spectroscopy, Leningrad 1962
21) H. Aeppli, H. Albers-Schönberg, H. Frauenfelder and P. Scherrer, Helv. Phys. Acta **25** (1952) 339
22) H. Albers-Schönberg, E. Heer, T. B. Novey and P. Scherrer, Helv. Phys. Acta **27** (1954) 547
23) R. M. Steffen and W. Zobel, Phys. Rev. **103** (1956) 126